Watkins-Johnson Company
Tech-notes

Vol. 11 No. 2 March/April 1984

PSK Demodulation (Part 1)

J. Mark Steber

Developed during the early days of the deep space programs, phase-shift keying now finds widespread use in both military and commercial communication systems. For telemetry applications, PSK is considered an efficient form of data modulation because it provides the lowest probability of error for a given received signal level, when measured over one symbol period. Terrestrial microwave radio links and satellite communication systems also frequently employ PSK as their modulation format.

The purpose of this tutorial is to outline the various practical techniques used for PSK demodulation. Relative relationships, such as tradeoffs between cost, complexity, and performance are also discussed. In addition, ample references are provided the reader for elaboration on selected topics.

Definitions

Phase-shift keying (PSK) is a modulation process whereby the input signal, a binary PCM waveform, shifts the phase of the output waveform to one of a fixed number of states. The signal can be written as

$$V_0(t) = \sqrt{2S}\ \mathrm{Sin}\left[\omega_0 t + \frac{2\pi(i-1)}{M}\right]$$

$i = 1,2,\ldots M$

$-T_s/2 \le t \le T_s/2$

where, S = the average signal power over the signaling interval, T_s, $\bar{\ }$

$M = 2^N$ the number of allowable phase states

N = the number of bits needed to quantize M

Three common versions, binary or BPSK (M=2), quadrature or QPSK (M=4), and 8ϕ PSK are described in Table 1.

The signal constellation is a pictorial representation of all possible signal states [1]. In each case, the transmitted signal is formed by appropriately weighting orthogonal carrier components. The weighting factor is such that the signals are constrained to lie on a circle of radius $\sqrt{E}$, where E is the transmitted signal energy. This constant-energy/constant-amplitude characteristic is important in satellite communication links where AM/PM conversion must be held to a minimum.

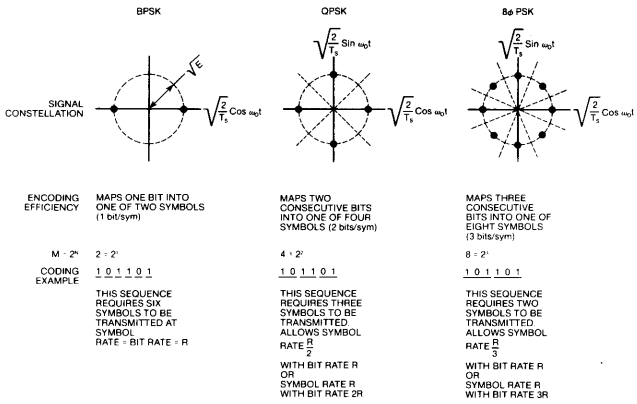

Table 1. Three common versions of phase-shift keying (BPSK, QPSK and 8ϕ PSK).

Again referring to Table 1, notice that QPSK and 8ϕ-PSK systems encode more hits of information per transmitted symbol than does BPSK. If a block of information must be transmitted over the same interval of time for all three cases, the signaling rate can be reduced in an M-ary system by a factor of N. And, since the maximum pulse rate (symbol rate) through a channel is proportional to its bandwidth, a reduced rate allows the use of narrower channels. Alternatively, if the symbol rate is held constant for all three cases, the higher-order systems transmit more bits of information through the fixed bandwidth channel. Therefore, M-ary systems are termed *bandwidth efficient.* The price to be paid for efficiency, however, is an increase in the system probability of error, since decisions as to which symbol was transmitted at any given time are now made in a more crowded signal space.

M-ary PSK may be characterized in the frequency domain by its spectral density, G(f), which is of the form

$$G(f) = A^2 T_s \left[\frac{\sin(\pi T_s(f-f_c))}{\pi T_s(f-f_c)} \right]^2 \qquad [2]$$

where, $T_s = (\log_2 M)\, T_b$ the symbol period

$1/T_b$ = the bit rate

f_c = the carrier frequency

A^2 = a constant proportional to average power

BPSK and QPSK spectra are compared on an equal bit-rate basis in Figure 1. Note that in both cases the spectrum is continuous; i.e., there are no discrete spectral lines, and there are nulls at multiples of the symbol rate.

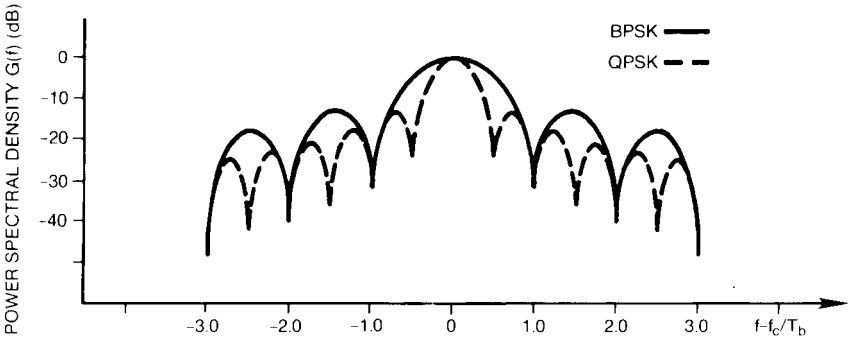

Figure 1. BPSK and QPSK spectra.

PSK Modulation Techniques

Although this article is concerned primarily with demodulation techniques involved in PSK systems, it will be helpful to also consider the encoding or modulation process. A typical BPSK modulator is shown in Figure 2.

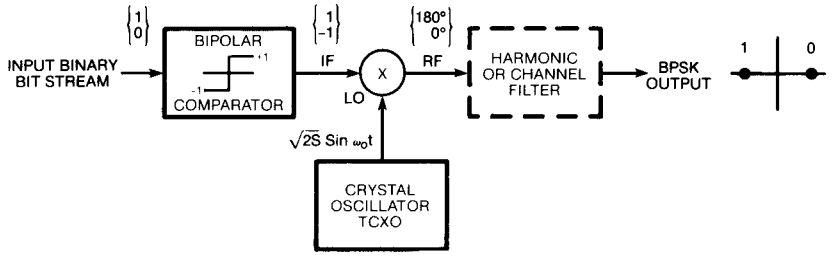

Figure 2. BPSK modulator.

The incoming unipolar waveform is converted to bipolar form, and switches current into and out of the IF port of a double-balanced mixer. Switching current in this fashion effectively imparts a 0° or 180° phase shift to the LO signal, $\sqrt{2}S \sin \omega_o t$. At this point the waveform is ready for amplification and transmission, but sometimes is filtered to minimize intersymbol interference. This filtering will be discussed in a later section.

A block diagram for a QPSK modulator is shown in Figure 3.

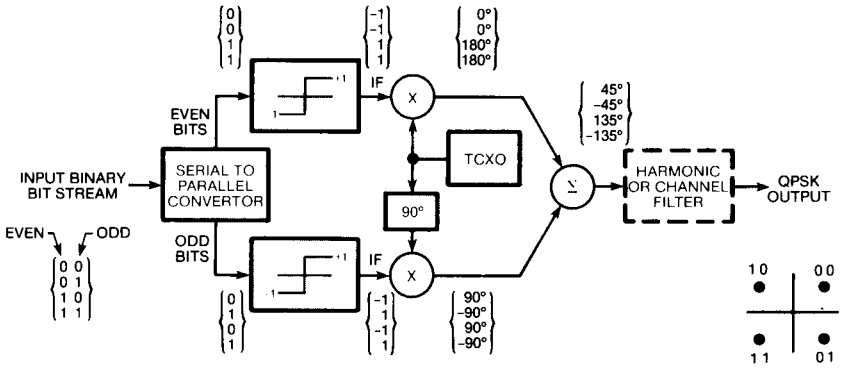

Figure 3. QPSK modulator.

PSK Demodulation

The demodulation process can be divided into three major subsections, as shown by Figure 4. First, since the incoming waveform is suppressed carrier in nature, coherent detection is required. The methods by which a phase-coherent carrier is derived from the incoming signal are termed, *carrier recovery,* and will be covered first. Next, the raw data are obtained by coherent multiplication, and used to derive clock-synchronization information. The raw data are then passed through the channel filter, which shapes the pulse train so as to minimize intersymbol-interference distortion effects. (The channel filter is sometimes placed at the IF input of the demodulator with equivalent results.) This shaped pulse train is then routed, along with the derived clock, to the data sampler which outputs the demodulated data.

The demodulated data will still exhibit an Mth-order ±180° phase ambiguity which must be corrected. The most common correction scheme calls for the transmission of a known sequence as a data preamble. After preamble decoding, the demodulator then inverts the bit streams that are in error.

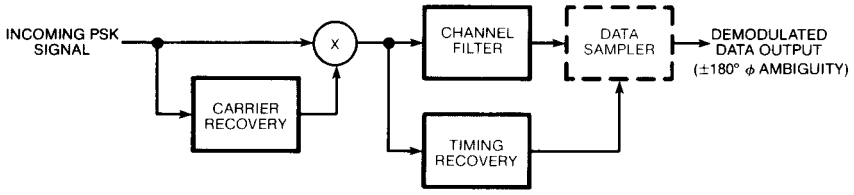

Figure 4. Block diagram of a PSK demodulator.

Carrier Recovery

The Costas Loop

The conventional Costas loop for BPSK suppressed carrier recovery is shown in Figure 5. Analysis of operation is lengthy and complex; the reader is referred to the many papers by Lindsey and Simon who developed much of the original work [3,5,6,8]. In keeping with their notation, the input signal can be expressed as

$x(t) = \sqrt{2S}\, m(t) \sin \phi(t) + n(t)$

where, S = the average received signal power

m(t) = the data modulation (±1 bipolar digital waveform)

$\Phi(t) = \omega_o t + \theta(t)$ the received signal phase

n(t) = additive channel noise

$\hat{\Phi}(t) = \omega_o t + \theta(t)\hat{}$ the VCO phase estimate

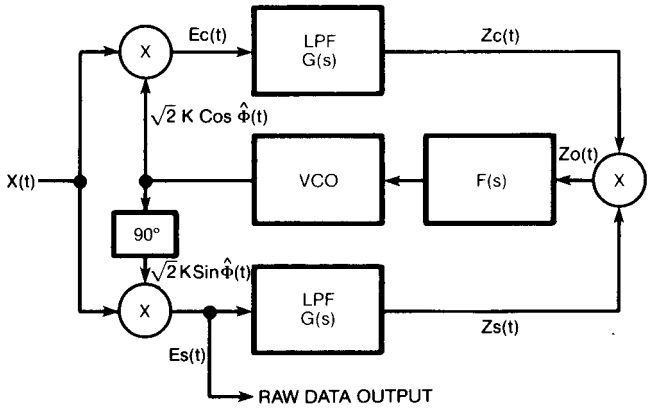

Figrue 5. Conventional Costas loop.

The Costas loop performs both phase-coherent suppressed carrier reconstruction and synchronous data detection within the loop. The upper loop is referred to as the quadrature, or tracking loop, and functions as a typical PLL, providing a data-corrupted error signal, $Z_c(t)$. The lower in-phase, or decisioning loop provides data extraction at the output of the lower mixer, and corrects the data corruption of $Z_c(t)$. The corrected error signal, $Z_o(t)$, is applied through loop filter F(s) to the VCO, which yields a phase estimate in the form cos $\Phi(t)$.

It can be shown that the Costas loop tracks a doubled phase error signal in the form

$\varepsilon(t) = Z_o(t)\, \alpha \sin 2\, \phi(t)$

with $\phi(t) = \Phi(t) - \Phi(t)$

The variance of the doubled error tracking jitter $\sigma_{2\phi}^2$ is used for cycle-slipping calculations, while σ_ϕ^2 is used in bit error-rate calculations.

Much work has been done describing the *linear* PLL model, and for many carrier tracking analyses this model will suffice. Out of this work, a fundamental expression relates the mean-squared phase-error jitter to the SNR "in the loop":

$\sigma_{2\phi}^2 = 1/\rho \ (\text{rads})^2 \qquad \rho = S/N_o B_L \qquad [4]$

For a 2nd-order PLL with loop filter,

$$F(j\omega) = \frac{1 + j\omega\tau_2}{j\omega\tau_1}$$

$$\sigma_\phi^2 = \frac{N_o}{A^2}\frac{\omega_n}{4\zeta}(1 + 4\zeta^2) = \left(\frac{S}{N_i}\right)^{-1}\frac{B_L}{B_i}$$

where, σ_ϕ = the rms phase jitter (rads)

$$\frac{S}{N_i} = \text{input SNR} \frac{A^2}{2N_oB_i}$$

B_L = one-sided loop bandwidth

B_i = double-sideband, one-sided IF bandwidth

This final expression is often used to determine loop bandwidths. Since carrier tracking can be optimized for a linear PLL by the adjustment of loop parameters, it is advantageous to analyze and specify the tracking performance of suppressed-carrier loops in the same way. Again, Lindsey and Simon have connected the two by an interesting relationship termed, *squaring loss* [5].

$\sigma_{2\phi}^2 = 4/\rho \ S_L$

$\sigma_\phi^2 = S_L^{-1}/\rho$

where, ρ = loop SNR $S N_oB_L$,
S_L = squaring loss

The term squaring loss (SL) is used to describe the degradation in loop SNR due to signal x noise and noise x noise distortion occurring in the arm filters. Dependent on the modulation format, input SNR, and filter type and bandwidth, the SL is quite difficult to calculate, even using simplifying expressions developed in [6]. Suffice it to say that as a practical matter, for uncoded systems, where E/N_o>10 dB, there is little to be gained by implementing arm filters more complex than Butterworth 2 poles, which result in an SL of a couple of dB.

To put things into perspective, Table 2 catalogs some of the more important aspects of tracking performance.

MEAN SQUARED PHASE JITTER $= \sigma_\phi^2 = \frac{1}{\rho} < \sigma_\phi^2 = \frac{1}{S_L \rho}$

CARRIER TRACKING LOOP — SUPPRESSED CARRIER TRACKING LOOP

SL DEPENDENT ON:
- DATA FORMAT; e.g., NRZ, MANCHESTER, ETC.
- SYMBOL RATE
- INPUT SNR (E/N_o)
- ARM FILTER TYPE, ORDER, BANDWIDTH

INTERRELATIONSHIPS

LOOP BANDWIDTH ↑ ACQUISITION TIME ↓ PHASE JITTER ↑ PROBABILITY OF ERROR P(e) ↑

Table 2. Tracking performance.

Costas Loop Variations

The Polarity Loop

Figure 6 shows a very common implementation called the hard-limited, or polarity loop.

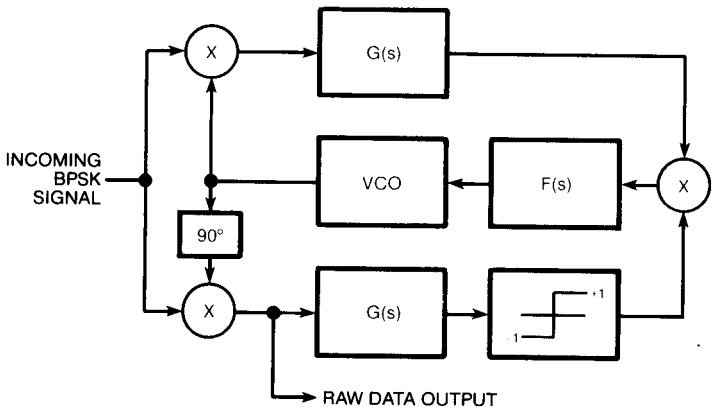

Figure 6. Hard-limited or polarity loop.

Ritter has shown that the optimal phase estimator requires a

$$\tanh\left(K \frac{E}{N_o}\right)$$

nonlinearity following the in-phase data arm filter. For large values of its argument, tanh (x) equals the polarity or sign of x (±1), and can be implemented with a hard limiter [7].

Simon has shown [8] that the inclusion of a limiter introduces a signal suppression factor into the analysis which can improve or degrade performance. Results indicate that for higher E/N_o ratios, there is an actual improvement in the loop's squaring loss. Also, inclusion of the limiter allows the substitution of a switching chopper multiplier for the analog (four quadrant) third multiplier, with its inherent dc-drift stability improvement.

A modified (hard-limited) Costas loop used for the demodulation of QPSK signals is shown in Figure 7. Not shown, is the required block that is used to interleave the two bit streams and resolve any ±180° phase ambiguities.

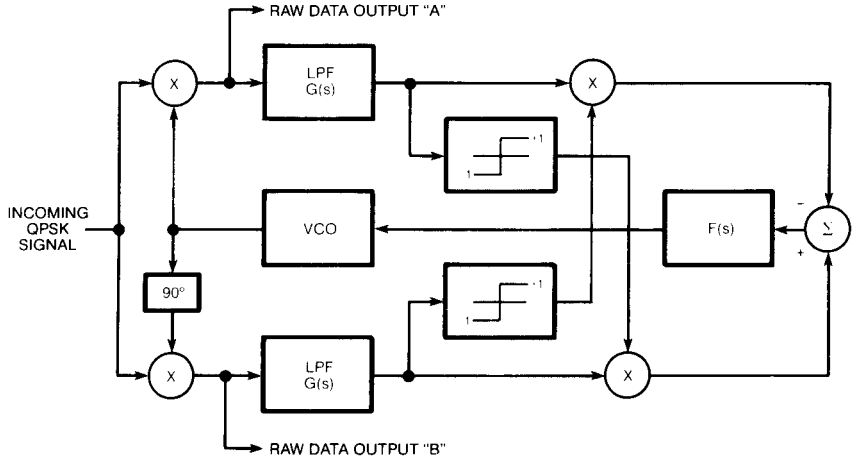

Figure 7. Modified (hard-limited) QPSK Costas loop.

The Remodulator

Another popular carrier recovery technique is called remodulation, and a BPSK implementation is shown in Figure 8.

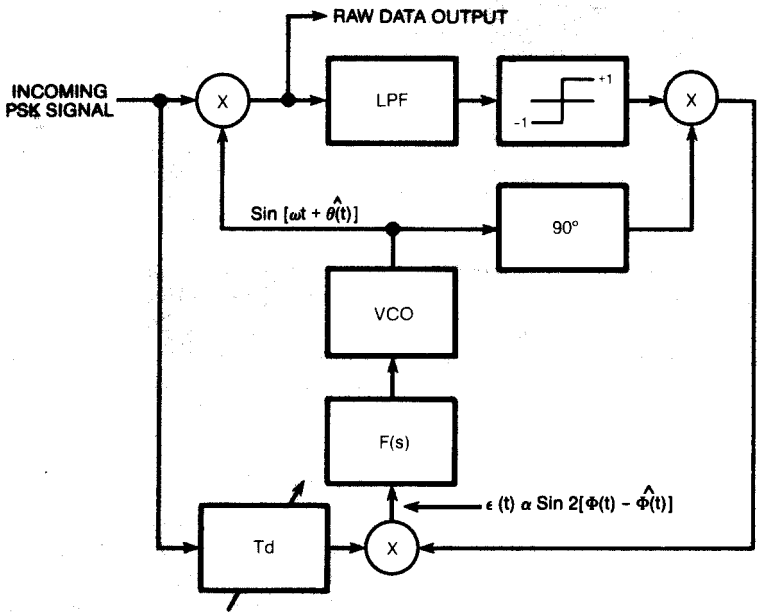

Figure 8. BPSK remodulator loop.

Again, as in the Costas loop, the remodulator generates a loop error signal proportional to the doubled phase error between incoming phase and its estimate; i.e.,

$\varepsilon(t) \alpha \sin 2[\Phi(t) - \hat{\Phi}(t)]$

It can be shown that the remodulator is stochastically equivalent to the polarity loop; i.e., hard-limited Costas loop. The remodulator, however, is typically implemented at frequencies lower than IF. This allows a digital (baseband) hardware realization, resulting in a low-cost demodulator.

A remodulation technique for QPSK carrier recovery and data extraction is shown in Figure 9. This version of the QPSK remodulator loop can be shown to be stochastically equivalent to the modified QPSK Costas loop described earlier [8, 9]. Weber has developed an expression for the remodulator S curve, g(ϕ), the equivalent loop nonlinearity. For high SNR, the phase-detector error characteristic approaches a sawtooth with four stable lock points at 0°, 90°, 180° and 270°. This sawtooth ensures a rapid transition between lock points, minimizing the lingering hangup effect sometimes occurring in a conventional Costas loop, due to its sin ϕ S-curve response. Therefore, the QPSK remodulator loop should exhibit a somewhat faster acquisition time when compared to a conventional QPSK Costas loop.

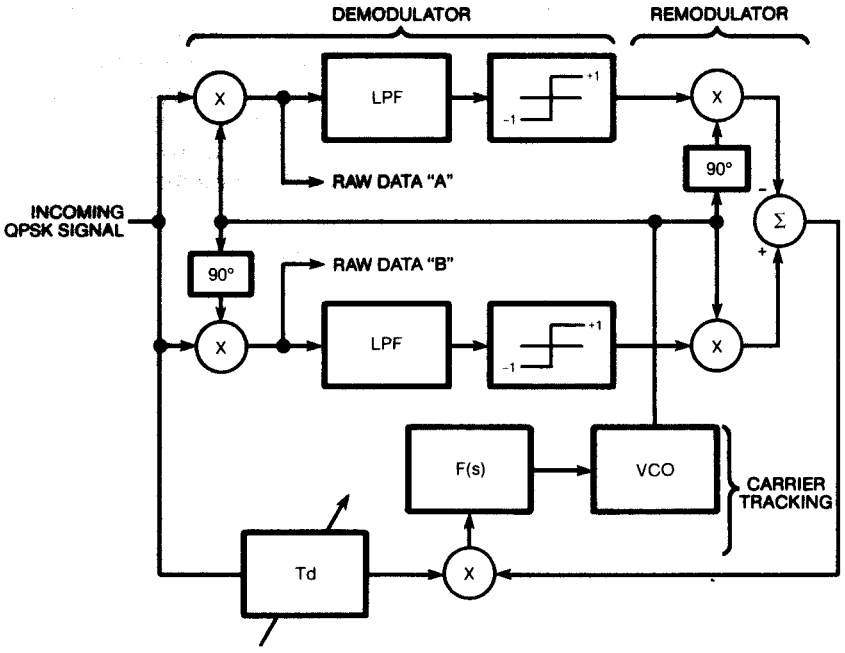

Figure 9. QPSK remodulator loop.

Multiply-Filter-Divide

Another method of QPSK carrier recovery used in high-rate, burst-mode systems is that of the multiply-filter-divide circuit shown in Figure 10.

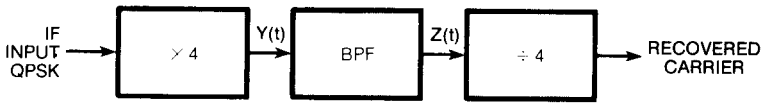

Figure 10. Multiply-filter-divide method of carrier recovery.

Consider the output of the 4th-order nonlinearity y(t)

$$y(t) = [x(t)]^4 \qquad x(t) = \sin\left[\omega_0 t \pm \frac{2\pi-(i-1)}{4}\right]$$

$$i = 1,2,3,4$$

By trigonometric identity (assuming *ideal* quadrupling)

$y(t) = 3/8 - 1/2 \cos [2 \omega_o t + \pi(i-1)] + 1/8 \cos [4 \omega_o t + 2\pi(i-1)]$

The filtered output, z(t), contains the desired harmonic at $f = 4f_{IF}$, with phase zero (modulo 2π). Frequency division by four yields the desired coherent carrier component. Tracking jitter is determined largely by the BPF's suppression characteristics [10].

Conclusion

The second part of this article will cover the other two subsections of a PSK demodulator: the symbol timing-recovery circuitry and the channel filter. In addition, bit error rate (BER) performance will be discussed and a method of measurement will be suggested.

Selected PSK Bibliography

1. Schwartz, M. Information Transmission, Modulation, and Noise, McGraw Hill, New York, 1980.

2. Feher, K., Digital Communications with Microwave Applications, Prentice Hall, New Jersey, 1981.

3. Lindsey. W. C. and Simon, M. K., Telecommunication Systems Engineering, Prentice Hall, New Jersey, 1973.

4. Blanchard, A., Phase Locked Loops, Wiley, New York, 1976,

a. Simon, M. K., and Lindsey, W. C., "Optimum Performance of Suppressed Carrier Receivers with Costas Loop Tracking," IEEE Transactions on Communications, VOL COM-25, No. 2 (Feb. 1977) pp. *215-227.*

6. Simon, M. K., "On the Calculation in Costas Loops with Arbitrary Arm Filters," IEEE Transactions on Communications, VOL COM-26, No. 1 (Jan. 1978) pp. 179-183.

7. Ritter, S., "An Optimum Phase Reference Detector for Fully Modulated Phase-Shift Keyed Signals," IEEE Transactions on Aerospace and Electronic Systems, VOL AES-5, No.4, July1969, pp. 627-631.

8. Simon, M. K., "Tracking Performance of Costas Loops with Hard-Limited In Phase Channel," IEEE Transactions on Communications, VOL COM-26, No, 4, April1978, pp. 420-432.

9. Weber, C. L., "Demod-Remod Coherent Tracking Receiver for QPSK and SQPSK," IEEE Transactions on Communications, VOL COM-28, No. 12, Dec. 1980, pp. 1945-1953.

10. Wolejsza, C. J., and Chakraborty, D., "TDMA Modem Design Criteria," Comsat Technical Review, Volume 9, Number 2A, Fall 1979.

11. Holmes, J. K., Coherent Spread Spectrum Systems, Wiley, New York, 1981.

12. Le-Ngoc, T., and Feher, K., "A Digital Approach to Symbol Timing Recovery Systems," IEEE Transactions on Communications, VOL COM-28, No. 12, Dec. 1980, pp. 1993-1999.

13. Lindsey, W. C., "A Survey of Digital Phase Locked Loops," Proceedings of the IEEE, VOL 69, No. 4, April 1981, pp. 410-430.

14. Cessna, J. R., and Levy, D. M., "Phase Noise and Transient Times for a Binary Quantized Digital Phase-Locked Loop in White Gaussian Noise," IEEE Transactions on Communications, VOL COM-20, No. 2, April 1972, pp. 94-104.

15. Texas Instrument Applications Report, Bulletin SCA-206, "Digital Phase-Locked Loop Design using

5N54/74L5297."

16. Mueller, K, H., "A New Approach to Optimum Pulse Shaping in Sampled Systems Using Time-Domain Filters, "BSTJ, VOL 52, No. 5, May-June 1973, pp. 723-729.

17. Feher, K., and DeCristofaro, R., "Transversal Filter Design and Application in Satellite Communications," IEEE Transactions on Communications, VOL COM-24, No. 11, Nov. 1976, pp. 262-1268.

18. Oppenheim, A. V., and Schafer, R. W., Digital Signal Processing, Prentice Hall, New Jersey, 1975.

19. Feher, K., Digital Communications — Satellite Earth Station Engineering, Prentice Hall, New Jersey, 1983.

20. Wozencraft, J, M. and Jacobs, I. M., Principles of Communication Engineering, Wiley, New York, 1965.